Polyamide–Imide Membranes with Surface Immobilized Cyclodextrin for Butanol Isomer Separation via Pervaporation

Yan Wang, Tai Shung Chung, and Huan Wang
Dept. of Chemical and Biomolecular Engineering, National University of Singapore, 4 Engineering Drive 4, Singapore 117576

DOI 10.1002/aic.12360
Published online August 3, 2010 in Wiley Online Library (wileyonlinelibrary.com).

A novel cyclodextrin (CD) derivative, m-xylenediamine-β-cyclodextrin (m-XDA-β-CD), has been synthesized and used to graft β-CD on membrane surface for the pervaporation separation of butanol isomers. The reaction mechanisms for the m-XDA-β-CD synthesis and the membrane surface grafting are confirmed by FTIR and TGA. The as-fabricated novel CD-grafted polyamide-imide (PAI) membranes show homogeneous morphology and significant improved separation performance as compared to the unmodified PAI membranes and PAI/CD mixed matrix membranes made of physical blends. The effects of chemical modification time and dope concentration on the asymmetric membrane have been studied. The optimal separation performance can be found with the CD-grafted PAI membrane cast from a 22 wt % dope concentration, which exhibits a total butanol flux of 15 g/m^2/h and a separation factor of 2.03. This newly developed membrane with surface-immobilized CD may open new perspective for the development of next-generation high-performance pervaporation membranes for liquid separations. © 2010 American Institute of Chemical Engineers *AIChE J,* 57: 1470–1484, 2011
Keywords: membrane separation, pervaporation, surface grafting, butanol isomer, cyclodextrin

Introduction

The separation of organic liquid isomers is a complex and challenging process in chemical industries as compared to other liquid mixtures, because of the similar physicochemical properties of the isomers. This topic has received a worldwide attention since 1980s owing to its scientific importance and high demands from chemical and pharmaceutical industries. However, isomer separation is poorly achieved by the conventional distillation process due to the similar volatility of the mixture pairs.[1] Low-temperature crystallization or adsorption processes are often used in the industry for isomer purification, but these processes are complex, expensive, and energy intensive.[2]

Among all these separation technologies, membrane-based pervaporation emerges as a promising technology recently, with many advantages unsurpassed by conventional technologies, like distillation, adsorption, extraction, crystallization, chromatography, etc. Membrane-based technologies provide numerous advantages such as appreciable energy savings, environmentally benign and clean technology with easy operation and easy scale-up with a small footprint. In addition to its attractive energetic efficiency, pervaporation itself carries special separation capabilities since the separation efficiency is mainly dependent on the differences in solubility and diffusivity of the penetrant pair with the membrane. Thus, a separation factor higher than the relative volatility in distillation can be achieved in pervaporation.

Correspondence concerning this article should be addressed to T. S. Chung at chencts@nus.edu.sg.

Table 1. Previous Studies on Pervaporation Separation of Isomers Through Polymeric Membranes

Feed Composition (Mass Ratio, wt %)	Membrane	Separation Factor (α)	Flux ($kg/m^2/h$)	T (°C)	Reference
p-/*m*-xylene (unknown)	Poly(vinylidene fluoride), Kynar@, Pennwalt	1.14	0.01	98	2
	Nylon, Allied Chemical, Capron@ 77C, 25 μm	1.22	0.01	120	
	Cellulose acetate, lOOCA-43, DuPont, 25 μm	1.45	0.02	98	
	Saran Wrap@, Dow, purchased locally, 20 μm	1.21	0.31	49	
	Poly(vinyl fluoride) Tedlar@, lOOAG3OUT, DuPont	1.16	0.01	81	
p-/*o*-xylene (unknown)	Poly(vinyl fluoride) Tedlar@, lOOAG3OUT, DuPont	1.33	0.02	72	
	Cellulose acetate, lOOCA-43, DuPont	1.56	0.01	81	
	Nylon, Allied Chemical, Capron	1.42	0.01	128	
	Saran Wrap@, Dow	1.26	0.08	49	
Unknown	Polyethylene	1.37	0.13	31	3
	Polypropylene	1.25	1.30	67	
p-/*o*-xylene (50:50)	Polycrystalline zeolite MFI ZSM-5 membrane	0.94–0.957	0.16	26–75	4
p-/*m*-xylene 10:90	PVA/β-cyclodextrin (β-CD: 33 wt %) crosslinked by glutaraldehyde on PAN support	2.96	0.095	25	5
p-/*o*-xylene (50:50)	Copolyimides of 6FDA-6FpDA/4MPD with DABA	1.15–1.29	21.4–24.9*	65	6
	Copolyimides of 6FDA-6FpDA/4MPD with DABA (4:4:1) crosslinked with HMDA	1.47	1.5*	65	
n-/*t*-butanol (55:45)	Nafion-based membrane consisting of an ultrathin polyion complex layer containing β-CD on the surface	2.0	0.016	25	7
o-/*p*-xylene (50:50)	Polyurethane membrane	1.37	0.30	25	1
	Polyurethane-zeolite composite membrane	1.89	0.31	25	
n-/*t*-butanol (50:50)	PAI asymmetric membrane with grafted β-CD	2.63	0.004	60	This work
		2.03	0.015	60	

6FDA: 4,4′-(hexafluoro-isopropylidene)-diphthalic anhydride; 6FpDA: 4,4′-(hexafluoro-isopropylidene)-dianiline; 4MPD: 2,3,5,6-tetramethyl-1,4-phenylene-diamine; DABA: 3,5-diaminobenzoic acid; HMDA: hexamethylene diamine.
*The flux given here is the normalized flux with the unit $kg/\mu m/m^2/h$.

However, the separation of organic liquid isomers through ordinary polymer membranes by pervaporation is still very challenging because of their similarity in physical and chemical properties. Various polymeric membranes have been studied for pervaporation separation of isomers as shown in Table 1 but all exhibit very low separation performance.[1–7] In the solution-diffusion model, the separation performance of a liquid mixture through a membrane is determined by the solubility and diffusivity of permeants in the membrane. Because of the similarity in size, it is difficult to separate isomer molecules based on diffusivity. Positive application of their solubility difference is one of the strategies to facilitate separation. Therefore, one must molecularly design membrane materials with suitable architecture and affinity which can recognize and take advantages of the slight difference in solubility and other physicochemical properties of isomers to achieve a high separation.

To enhance the separation performance, mixed matrix membranes (MMM) containing cyclodextrin (CD) units such as poly(acrylic acid) (PAA)/CD or poly(vinyl alcohol) (PVA)/CD membranes have been investigated extensively by pervaporation separation for organic dehydration,[8,9] isomer separations,[5,7,10–13] and other organic–organic separations.[14,15] Experimental results showed that the CD addition increased the membrane separation performance in both permeation flux and selectivity due to the unique molecular recognition property of CD. Despite a hydrophilic outer surface, the presence of a hydrophobic cavity enables CD to entrap small hydrophobic molecules to form inclusion compounds without forming stable chemical bonds.[16] Such incorporation involves hydrophobic interaction, hydrogen bonding, van der Waals forces, or conformational relaxation of the CD ring.[11] Furthermore, the steric fit between the CD cavity and the guest molecules plays an important role in selective inclusion for CD to recognize the slight difference in isomers' structures.[11,17]

However, the inclusion of CDs in the polymeric matrix by simple physical mixing encountered the problem of phase separation because of the CD agglomeration especially in the case of high CD loadings.[18] The CD molecules may also dissolve into the aqueous feed solution, and lead to declined separation performance. Therefore, it is necessary to fabricate a pervaporation membrane with immobilized CD. Grafting CD on the membrane surface via some chemical bonds would be an effective way. Not only it may solve the phase separation problem in mixed matrix membranes and the CD leaching problem in aqueous feed solutions but also makes it applicable for various types of asymmetric membranes with increased flux compared with those dense membranes.

In this study, m-xylenediamine (m-XDA) modified CD, one kind of β-CD derivatives containing amino groups, is synthesized and used for the membrane surface modification. Aromatic polyamide-imide (PAI) is selected as the matrix material to be modified with CD grafting for the separation of *n*-butanol/*tert*-butanol isomers via pervaporation. Compared to previously used materials, like PVA, PAA, etc., which are relatively weak in mechanical strengths and chemical resistance, PAI brings together superior mechanical properties typically associated with polyamides, and the high thermal and solvent stability of polyimide (PI), making it especially attractive for the pervaporation separation of aqueous organic mixtures. The PAI membrane has an advantage that suffers less from swelling in organic solvents and helps stabilize permselectivity in long-term operations. Several studies for alcohols dehydration have shown that PAI is a promising membrane material by pervaporation.[19–23] Another advantage of PAI is its unique compatibility with nano-particles,[24,25] which is highly advantageous for the fabrication of a defect-free PAI/CD MMM membrane. However, very limited studies[18,26,27] have been reported. Therefore, we aim to study the science of grafting CD onto PAI asymmetric membranes and investigate its

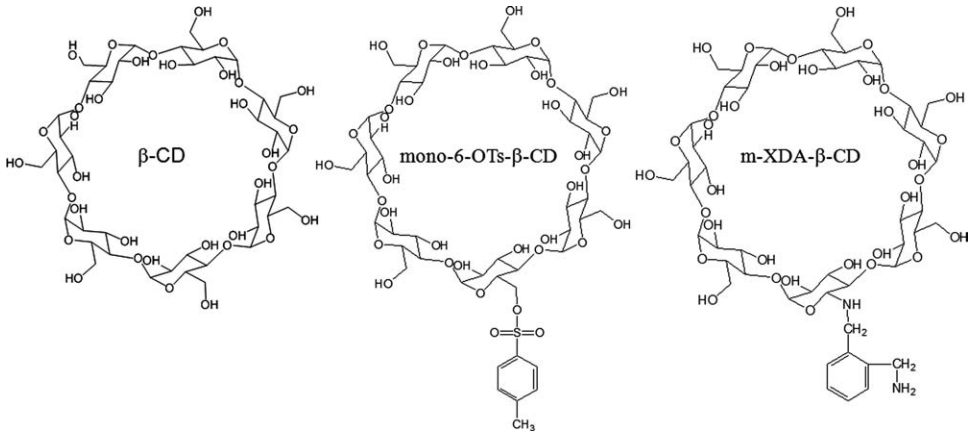

Figure 1. The chemical structures of β-CD and its derivatives: mono-6-OTs-β-CD and m-XDA-β-CD.

potential to separate butanol isomers by pervaporation. The effects of surface modification conditions, dope concentration to prepare membranes on the pervaporation performance of the resultant CD-grafted PAI membrane will be systematically investigated.

Experimental

Materials

The PAI used is Torlon® 4000TF polyamide-imide purchased from Solvay Advanced Polymers. The chemical structure of Torlon 4000T was reported by Robertson et al according to a NMR spectroscopy study.[28] 6-O-monotosyl-β-cyclodextrin (mono-6-OTs-β-CD) was purchased from Cyclolab and used as the precursor for the CD modification. Figure 1 shows their chemical structures. Both the polymer PAI and CD were dried overnight at 120°C under vacuum before use.

M-xylenediamine (m-XDA), used for the synthesis of the new CD derivative, m-xylenediamine-β-cyclodextrin (m-XDA-β-CD), is from Merck (Germany). *N*-methyl pyrrolidone (NMP), used as the solvent to prepare the membranes, was supplied by Merck with analytical grade and used as received. *n*-Butanol (*n*-BuOH) and *tert*-butanol (*t*-BuOH) were purchased from Tedia and Merck, respectively, with analytical grade and used as received.

Synthesis of m-XDA-β-CD

Figure 2 demonstrates the chemical route for the synthesis of m-XDA-β-CD from Mono-6-OTs-β-CD.[29,30] Typically, 5 g of Mono-6-OTs-β-CD was reacted with excess amount (30 ml) of m-XDA at 75°C for 4 h. After the reaction was completed, the mixture was allowed to cool to room temperature, 30 ml of cold acetone was added to precipitate the m-XDA-β-CD produced. Since the precipitated m-XDA-β-CD formed a suspension in the solvent/nonsolvent mixture, a centrifuge (20,000 rp/min) was used to separate m-XDA-β-CD from the liquid. Thereafter, the acetone was drained off and the precipitates were dissolved in a 30 ml water/methanol (1:1) mixture. The above precipitation and dissolution procedure was repeated several times to remove un-reacted m-XDA. The sample separated in the last cycle of wash was dried at 50°C for 3 days in vacuum, and m-XDA-β-CD was obtained with the yield of around 20 to 80 wt %. The detailed chemical structure of synthesized m-XDA-β-CD is also shown in Figure 1.

Membrane fabrication and surface modification with grafted CD

Dense flat-sheet membranes were fabricated by using a 15 wt % PAI solution in NMP. The solution was allowed to degas overnight prior to casting onto a glass plate with a casting knife at a thickness of about 100 μm. The as-cast membrane was then placed on a hot plate preheated at 75°C for 18 h. The solvent was slowly evaporated and the resultant film was carefully peeled off and placed between two wire meshes. Then, the membrane was dried under vacuum with temperature gradually increasing to 250°C at a rate of 12°C/20 min, hold there for 24 h to remove the residual solvents, and then allowed to cool to room temperature naturally. The wire meshes not only prevent the membrane from sticking to the glass plate but also help uniformly dry the membrane from both surfaces. The

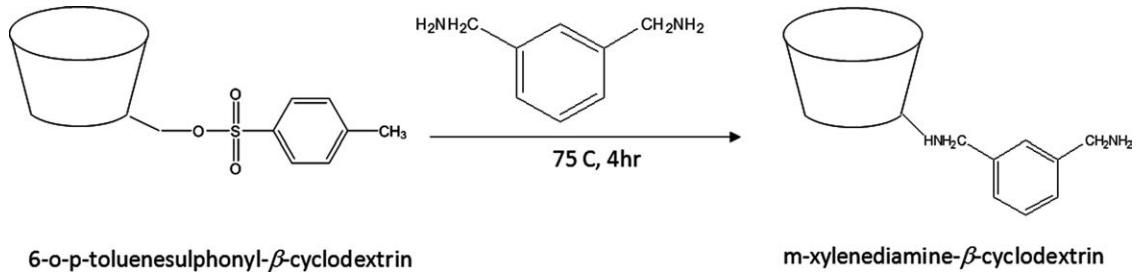

Figure 2. The reaction mechanism of m-XDA-β-CD synthesis.

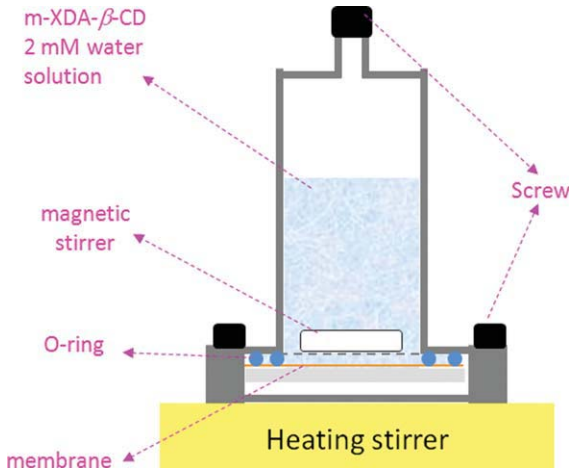

Figure 3. The schematic diagram of a lab-scale set-up for the surface modification of the flat-sheet membrane with m-XDA-β-CD.

[Color figure can be viewed in the online issue, which is available at wileyonlinelibrary.com.]

thickness of the dense flat membrane was around 10–15 μm measured by a Mitutoyo micrometer.

For the asymmetric membrane, NMP was also used as the solvent to dissolve the polymer completely at a certain high concentration (18 wt % and above). Similarly, the solution was also degassed overnight before casting onto a glass plate with a casting knife at a thickness of about 250 μm. The as-cast membrane was then immersed into a water coagulation bath at room temperature immediately and left in the water bath for 3 days with water changed daily. The as-cast asymmetric membranes were then dried in a Freeze-dryer (Thermo Electron, ModulyoD-230) with vacuum overnight after frozen in a fridge for 2 h.

After the membrane was fabricated, surface modification with a 2 mM m-XDA-β-CD/water solution was carried out on the membrane surface using a lab-scale apparatus (Figure 3) at room temperature for varied times. The proposed mechanism for the conjugation of m-XDA-β-CD onto the PAI membrane and the formation is represented schematically in Figure 4.

Pervaporation study

Pervaporation tests were conducted using a laboratory bench test unit supplied by Sulzer Chemtech GmbH and its design has been described elsewhere.[31] A two-liter feed solution of *n*-BuOH/*t*-BuOH of 50/50 wt % was circulated on the top of the membrane with a recirculation rate of 80–85 l/h. The bottom surface of the membrane (i.e., the downstream) was under vacuum which was generally kept less than 0.5 kPa. The employed Sulzer-made pervaporation cell for membrane permeation tests was about 15.2 cm^2 in area. The operational temperature was controlled by a heating bath at 60°C. Permeate samples were collected by a cold trap immersed in liquid nitrogen after 2-h conditioning of the pervaporation operation. The feed content varied less than 0.5 wt % during the entire experiment. Therefore, the feed concentration may be considered as a constant during the entire experiment because of the large quantity of the feed solution compared to the permeate sample.

The flux was determined by the mass of permeate divided by the product of the interval time and membrane area. The mass of permeate was weighed using a Mettler Toledo balance. The separation factor α is defined by the equation below:

$$\alpha = \frac{y_1/y_2}{x_1/x_2} \tag{1}$$

where subscripts 1 and 2 are the two components in the binary system, *y* and *x* are their corresponding weight fractions in the permeate and feed, which can be analyzed through a Hewlett-Packard GC 7890 with a HP-INNOWAX column (packed with cross-linked polyethylene glycol) and a TCD detector.

Characterization of CDs and the membranes

FTIR (Fourier transform infrared spectroscopy) analyses of β-CD, its derivatives (mono-6-OTs- β-CD and m-XDA-β-

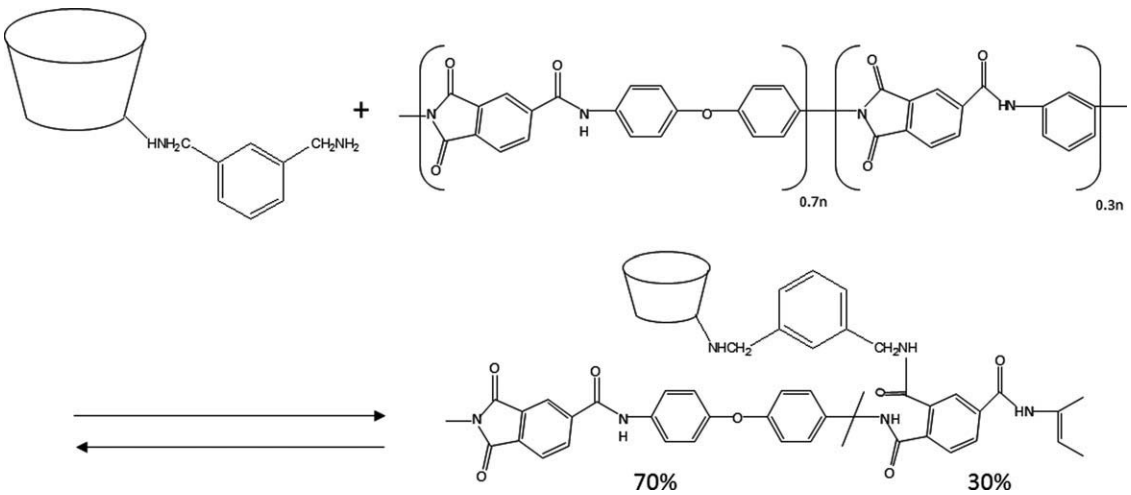

Figure 4. The reaction mechanism of the surface grafting of the flat-sheet membrane with m-XDA-β-CD.

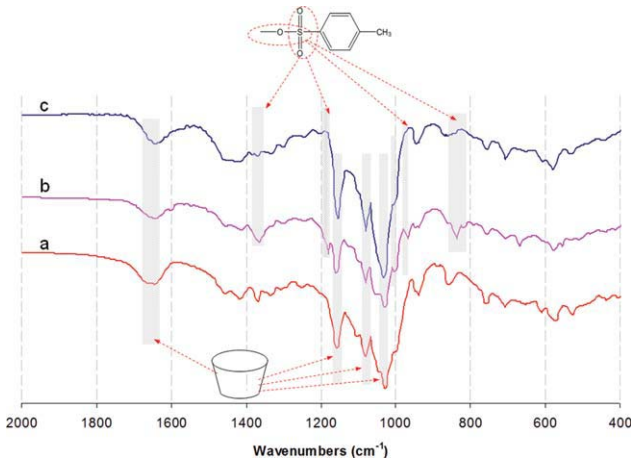

Figure 5. FTIR characterization of (a) β-CD, (b) mono-6-OTs-β-CD, and (c) m-XDA-β-CD.

[Color figure can be viewed in the online issue, which is available at wileyonlinelibrary.com.]

CD) as well as the membranes were performed using a Perkin–Elmer FTIR Spectrum 2000 with a resolution of 2 cm^{-1}. The spectra were obtained with an average of 16 scans. The thermal decomposition temperatures (T_ds) of CDs and membranes were characterized by thermogravimetric analysis (TGA) with a TGA 2050 Themogravimetric Analyzer (TA Instruments). The analysis was carried out with a ramp of 5°C/min at the temperature ranging from 50 to 800°C, under nitrogen atmosphere. The membrane morphologies of neat PAI and CD-grafted PAI-CD composite membranes were observed using a JSM-6700F field emission scanning electron microscope (FESEM). A Perkin Elmer Pyris-1 differential scanning calorimeter (DSC) was used to characterize the glass transition temperature (T_g) of the membranes using a heating rate of 20°C/min and N_2 purging of 25 ml/min. The T_g value is taken as the middle of the slope transition in the DSC curve. The solubility tests were carried by observing the membranes in the NMP solvent and taking photos of them after 10-min immersion to investigate their changes.

Computational simulation of the butanol inclusion in the CD cavity

All molecular modeling studies were performed using the Material Studio 4.1 software package developed by Accelrys. The initial structures of CD, butanols, and bound complexes were constructed and visualized using the builder module and were then optimized by a molecular mechanics technique to achieve the, respectively, minimized energy using the minimizer in the module of Amorphous Cell. The pcff force field and 5000 interations were used for all calculations.

Results and Discussion

Characterization of the synthesized m-XDA-β-CD as compared with mono-6-OTs-β-CD

The successful synthesis of the m-XDA-β-CD from the precursor, mono-6-OTs-β-CD, is confirmed by FTIR and TGA characterizations. Figure 5 shows the IR spectra of β-CD, mono-6-OTs-β-CD, and m-XDA-β-CD. Several IR peaks characteristic of typical CD units are clearly observed in all these three types of CD: O—H bending vibration[32,33] at about 1640 cm^{-1} and strong C—O—C characteristic stretching vibration[29,33] at around 1158, 1100, and 1030 cm^{-1}. A closer comparison of IR spectra of mono-6-OTs-β-CD and m-XDA-β-CD shows diminishments of the peaks at 1366, 1180, 968, and 838 cm^{-1}, which are ascribed to the asymmetric O=S=O stretching, symmetric O=S=O stretching and S—O—C stretching,[34] respectively. This demonstrates that the sulfonyl group is removed from the CD ring in the newly synthesized compound, as illustrated in Figure 2.

The TGA results of original β-CD, mono-6-OTs-β-CD, and synthesized m-XDA-β-CD are shown in Figure 6. The original mono-6-OTs-β-CD has a lower degradation temperature ($T_d \approx 160$°C), compared to a comparable high T_d (290°C) of the original β-CD. The synthesized m-XDA-β-CD has a T_d of about 240°C, much higher than mono-6-OTs-β-CD. This indicates the successful synthesis of a new compound, different from mono-6-OTs-β-CD.

Molecular simulation is an important tool to provide additional insights to elucidate the butanol inclusion in the CD cavity. Figure 7 illustrates the simulated structures before and after the inclusion of one *n*-BuOH molecule into the β-CD cavity. The initial energies of individual components as well as the final energy with the most stable inclusion structure are summarized with the aid of the Accelrys Material Studio software package. By subtracting the minimized energy of CD and butanol in the initial stage (i.e., both of them are separated) to that under the final stage (i.e., an inclusion state), we can estimate the energy drop during the butanol inclusion.[35] An energy drop of about 15.589 kcal/mol indicates that the inclusion of *n*-BuOH inside the cavity of β-CD is favorable to lower the total energy and thus to form a stable structure. The larger the energy drop, the more stable and easier of butanol inclusion into the CD.

To elucidate and compare the selective inclusion abilities of β-CD and m-XDA-β-CD for butanol isomers, the inclusions of one *n*-BuOH or *t*-BuOH molecule into β-CD and m-XDA-β-CD are simulated using this method. Figure 8 shows the top and side views of their chemical structures,

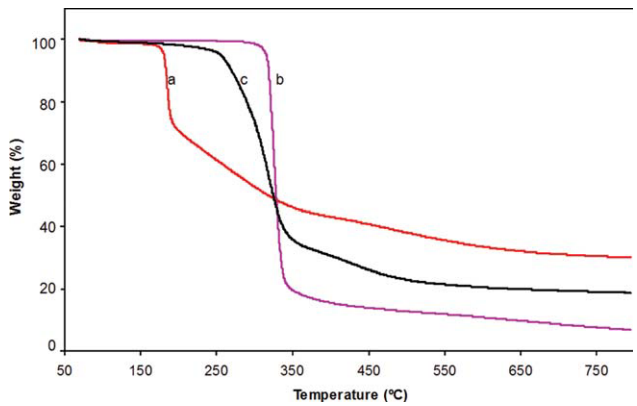

Figure 6. TGA characterization of (a) mono-6-OTs-β-CD, (b) β-CD, and (c) m-XDA-β-CD.

[Color figure can be viewed in the online issue, which is available at wileyonlinelibrary.com.]

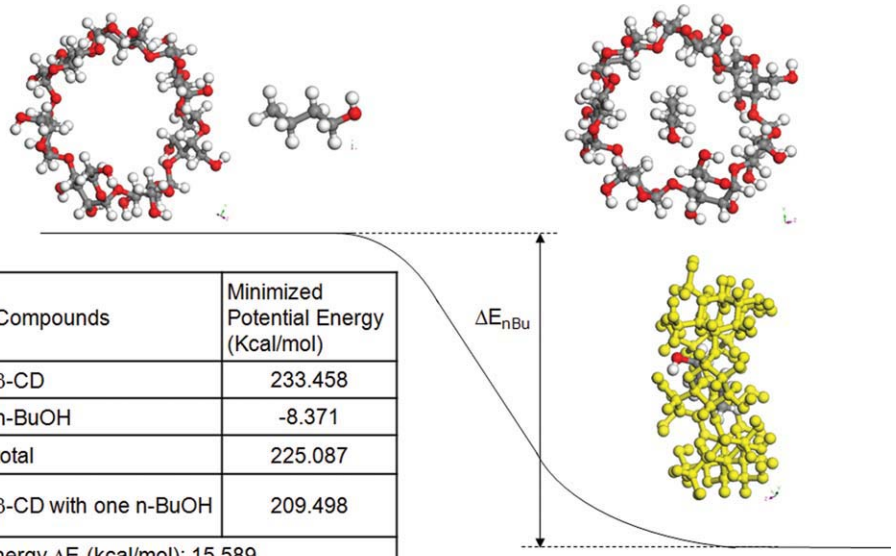

	Compounds	Minimized Potential Energy (Kcal/mol)
Initial stage	β-CD	233.458
	n-BuOH	-8.371
	total	225.087
Final stage	β-CD with one n-BuOH	209.498
Reduced energy ΔE (kcal/mol): 15.589		

Figure 7. Simulated structures before and after the inclusion of one *n*-butanol molecule into *β*-CD.

[Color figure can be viewed in the online issue, which is available at wileyonlinelibrary.com.]

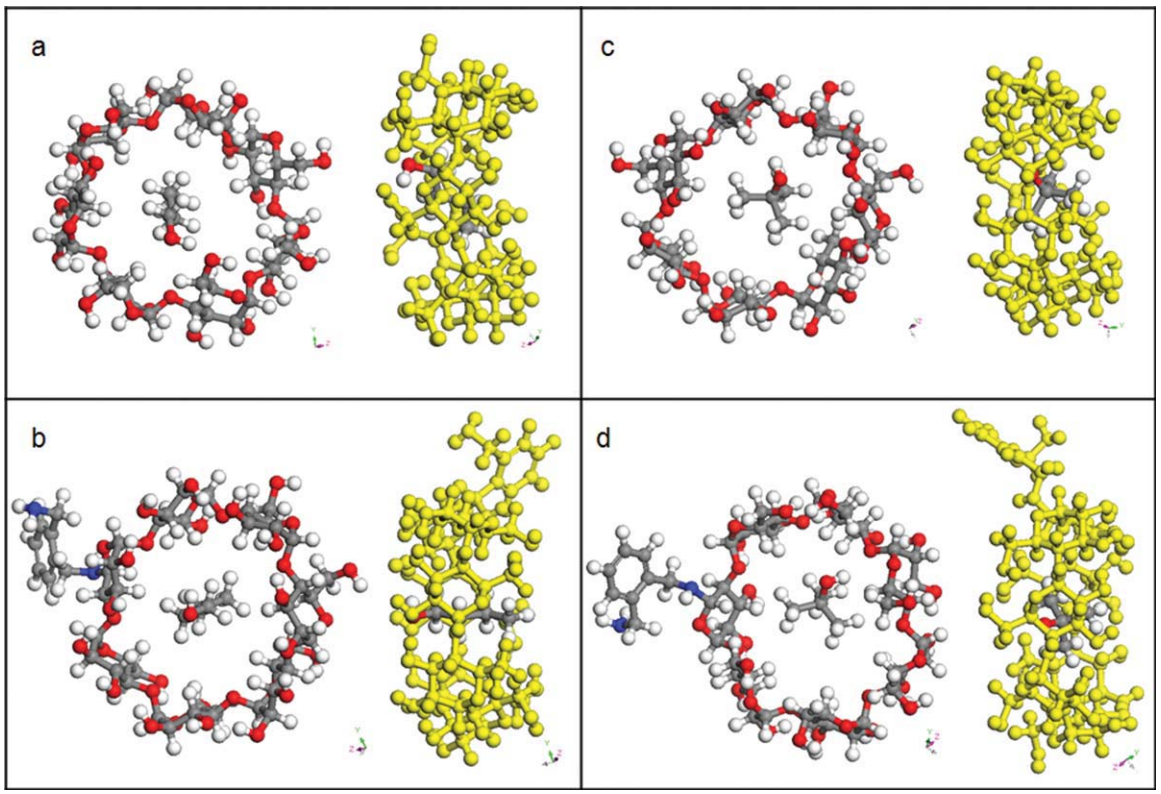

Figure 8. The top views and side views of the simulated structures after binding one *n*-butanol molecule with (a) *β*-CD and (b) m-XDA-*β*-CD; as well as one *tert*-butanol molecule with (c) *β*-CD and (d) m-XDA-*β*-CD.

[Color figure can be viewed in the online issue, which is available at wileyonlinelibrary.com.]

Table 2. Simulation Results of the Minimized Potential Energy Before and After the Butanol Inclusion Into β-CD and m-XDA-β-CD

	Each Molecule Before Insertion (kcal/mol)	Simulation	Total Energy Before Inclusion	Total Energy After Inclusion	Reduced Energy ΔE (kcal/mol)	ΔE_{n-BuOH}–ΔE_{t-BuOH}
n-butanol	−8.371					
t-butanol	−52.198					
β-CD	233.458	With *n*-BuOH	225.087	209.498	15.589	0.401
		With *t*-BuOH	181.260	166.073	15.187	
XDA-β-CD	222.623	With *n*-BuOH	214.252	200.367	13.886	1.861
		With *t*-BuOH	170.425	158.401	12.025	

and Table 2 summarizes their energy drops. The results show that the inclusion of *n*-BuOH in both CDs is of a larger energy drop than that of *t*-BuOH, indicating that the inclusion of the former in the cavity of both CD types is easier than the latter. In another word, both two CDs exhibit preferential sorption and/or diffusion selectivity toward *n*-BuOH. The results also show that the energy drops for both butanol inclusion in β-CD is larger than m-XDA-β-CD, indicating β-CD has larger butanol inclusion ability than m-XDA-β-CD, which is linked to a higher permeation flux of butanol isomer mixture.

As CD is used as the butanol selector in this study, one can deduce its discrimination ability for a pair of butanol isomers by comparing the difference in their energy drops. The last column of Table 2 tabulates these differences with a higher value of m-XDA-β-CD than that of β-CD. This implies that m-XDA-β-CD shows a greater selectivity for the *n*-butanol/*t*-butanol pair compared to that of β-CD. Of course, due to the complexity of the inclusion process of butanol molecules into CD cavity, the real situation may involve in partial or multiple butanol molecules inclusion in a β-CD molecule.[18] Nevertheless, the simulation results give us a basic understanding of their inclusion and discrimination abilities to the *n*-/*t*-BuOH isomer pair.

Comparison of the unmodified membranes with modified dense membranes

Up to the present, there are very limited studies on alcohol isomer separation by pervaporation.[7,11] Most previous studies on isomer separation by pervaporation have been focused on xylene isomers. One of the possible reasons may be due to the higher challenge compared to the separation of the xylene isomers because the molecular sizes of C_3—C_4 alcohols are smaller than xylene. The other reason is that the industrial process of xylene production does lead to a mixture of xylene isomers. Depending on feed composition and fermentation conditions, the industrial process of butanol production may also contain minor butanol isomers and other components such as acetone and acids. However, this study is intended to focus on a simple case: separation of butanol isomers as conceptual demonstration. The study of butanol isomer separation may bring insights for the pervaporation separation of other isomers, because of their small differences and easy availability of butanol isomers compared to xylene isomers. As shown in Table 3, only small differences of *n*-BuOH and *t*-BuOH isomers exist in their kinetic diameters, molecular volumes, polarity parameters [E_T (30)], and solubility parameters. The only significant and useful difference is in their average dynamic cross-section which is due to the fact that *n*-BuOH molecule is of a much higher linearity than the *t*-BuOH molecule. This linearity difference in the butanol isomers could be the breakthrough point to achieve the separation. So far, there is one study on the separation of propanol isomers through PVA/β-CD dense membranes[11] and one study on the separation of butanol isomers[7] by means of a charged Nafion-based membrane consisting of an ultrathin polyion complex layer containing β-CD on the surface. Both studies exhibited enhanced pervaporation selectivity for alcohol isomers, indicating the effectiveness of β-CD as a selectivity enhancer for the isomers. Therefore, in this study, PAI membranes with immobilized CD are investigated for butanol isomer separation.

Table 4 shows a comparison of pervaporation performance of the original PAI dense membrane, the mixed matrix membranes cast from physically blends of PAI and various CDs at 10 wt % CD loading,[18] and the CD-grafted PAI dense membrane after 5-h surface modification. Here, α- and γ-CD are another two common cyclodextrins with similar chemical structures of β-CD, and constituted by six and eight glucopyranoside units. Their chemical structures and basic properties are briefed in our previous study.[18] The CD-grafted PAI dense membrane has a higher separation factor for butanol isomers but with some sacrifice in flux. The obvious enhancement in separation factor from 1.11 of the original to 2.30 of the grafted is mainly attributed to the special molecular recognition ability of the CD compound and the uniform distribution of the CD units upon the membrane surface. As a result, the addition of

Table 3. The Physicochemical Properties of *n*-Butanol and *t*-Butanol[18]

Property Butanol	Boiling Points (°C)	Density (g/cm^3)	Molecular Weight (g/mol)	Molecular Volume (Å^3)[a]	Radius of Gyration (Å)[b]	Kinetic Diameter[36] (Å)	Average Dynamic Cross-Section[37]	E_T (30)[38] (kcal/mol)	Solubility Parameter[39] (J/cm^3)$^{1/2}$	Solubility in Water (25°C)
n-BuOH	117.8	0.810	74.1	151.8	3.251	5.05	1.22	49.7	23.1	9.1 ml/100 ml
t-BuOH	82.4	0.781	74.1	157.4	3.067	5.06	2.04	43.3	21.8	Very good
Difference				3.69%	6.00%	0.20%	67.21%	14.78%	5.96%	–

[a]The molecular volume is calculated by the molecular weight divided by the density and the Avogadro number.[40]
[b]The radii of gyration are calculated using Aspen DISTIL (version 2004.1).

Table 4. Pervaporation Performance of Different Dense PAI Membranes

Membrane Type	Total Flux ($g/m^2/h$)	Separation Factor (*n*-Butanol/*t*-Butanol)
Original PAI dense membrane[18]	8	1.11
PAI/α-CD mixed matrix membrane[18]	3	1.34
PAI/β-CD mixed matrix membrane[18]	10	1.30
PAI/γ-CD mixed matrix membrane[18]	22	1.13
CD-grafted PAI dense membrane (this work)	2.7	2.30

Feed composition: *n*-/*t*-butanol 50/50 wt %.
Operational temperature: 60°C.
Downstream pressure: <2 m bar.

CD on the membrane surface induces larger differences in sorption and/or diffusivity between *n*-BuOH and *t*-BuOH.

It is well-known that CD forms a complex more predominantly with an *n*-derivative than with a *t*-derivative owing to the steric effect.[17] Since *n*-butanol molecule has a linear shape and is much narrower than *tert*-butanol molecule, the ability of the former to transport through CD is much easier than that of the latter. In addition, *n*-BuOH is slightly more hydrophobic than *t*-BuOH according to their solubility parameters as shown in Table 3. As a result, the former can preferentially transport through the hydrophobic CD cavity compared to the latter because of higher diffusion selectivity in the CD-grafted PAI membrane. Similar results have been reported previously.[5,7,10–13,18] The simulation result also indicates that m-XDA-β-CD has a higher butanol selectivity than the original β-CD.

Compared to the PAI dense membrane and PAI-CD mixed matrix membranes made of physical blends, the flux reduction in the CD-grafted PAI membrane may arise from several factors: (1) the grafted CD molecules are distributed upon the membrane surface as a barrier or selective layer; (2) the embedding of bulky β-CD or γ-CD within the PAI matrix via physical blends may induces defects and creates by-pass channels to enhance flux;[26,27] (3) m-XDA-β-CD has lower inclusion ability (i.e., flow channel) compared to the original β-CD as disclosed by the molecular simulation; and (4) the m-XDA may have residuals left in the synthesized m-XDA-β-CD as shown in Figure 2, and induce cross-linking reactions with the PAI matrix as elucidated in Figure 9.

Since the m-XDA has a much smaller volume than m-XDA-β-CD, it has a faster reaction rate with the imide group of the PAI membrane, thus causing the membrane chains packing closer and denser, and reducing the permeation flux. Besides, some other factors may also have negative impacts on butanol permeation flux. For example, even though β-CD has a bigger cavity size of (6.0∼6.4 Å[41]) than the *d*-space (average intersegmental distance of polymer chains) of the Torlon® 4000TF PAI polymer chains (4.3 Å),[19] the cavity directions of grafted β-CD are random. The conical cavity may hinder flux when flow is from the big open to the small open. In addition, β-CD itself fills and occupies membrane space.

Figure 10 shows a morphological comparison of the grafted PAI membrane with PAI/CD MMM membranes embedded with 5 and 10 wt % of β-CDs.[18] Clearly, the surface morphology of the grafted PAI is uniform and homogenous. In contrast, the inhomogeneity is clearly observed for membranes embedded with the original β-CD. The high hydrophilicity of the β-CD outer surface is the major cause for the inhomogeneity because the PAI matrix is relative hydrophobic, which results in β-CD aggregation and formation of the micro-scale drop-let/matrix surface morphology.[27] Compared to β-CD, m-XDA-β-CD has only one hydroxyl group on the exterior of CD ring being substituted by the m-xylenediamine. Therefore, the outer surfaces of the CD derivative are supposed to be similarly hydrophilic to that of β-CD. The reason that PAI-CD composite membrane successfully avoids the problem of CD agglomeration is ascribed to the

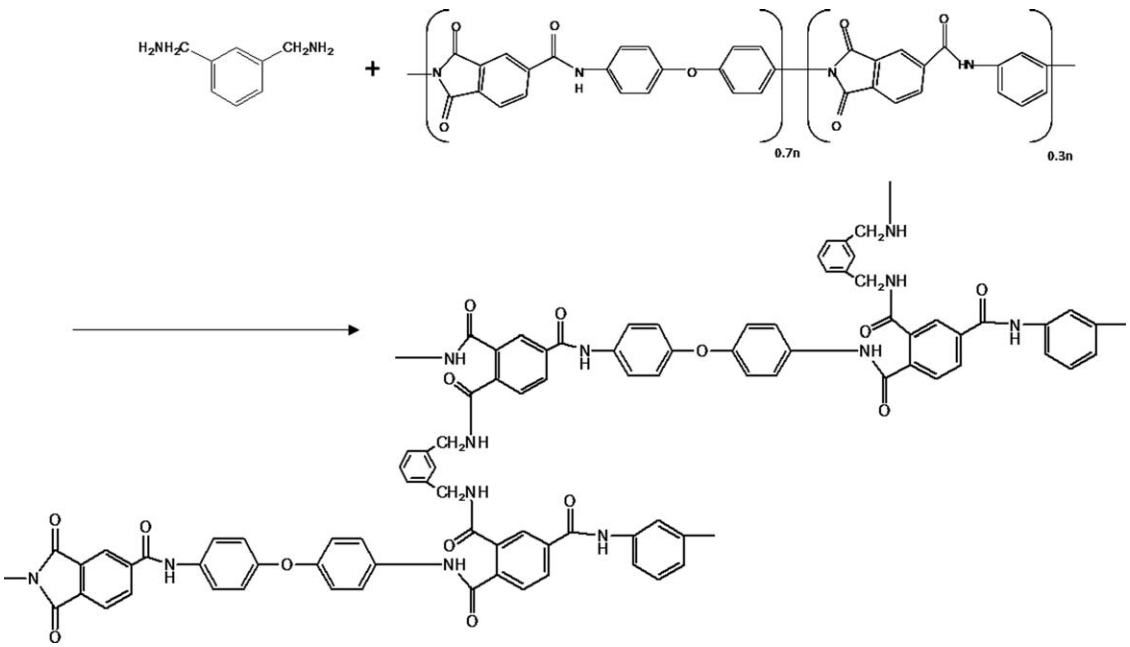

Figure 9. Possible cross-linking mechanism of PAI polymer chains by m-xylenediamine (m-XDA).

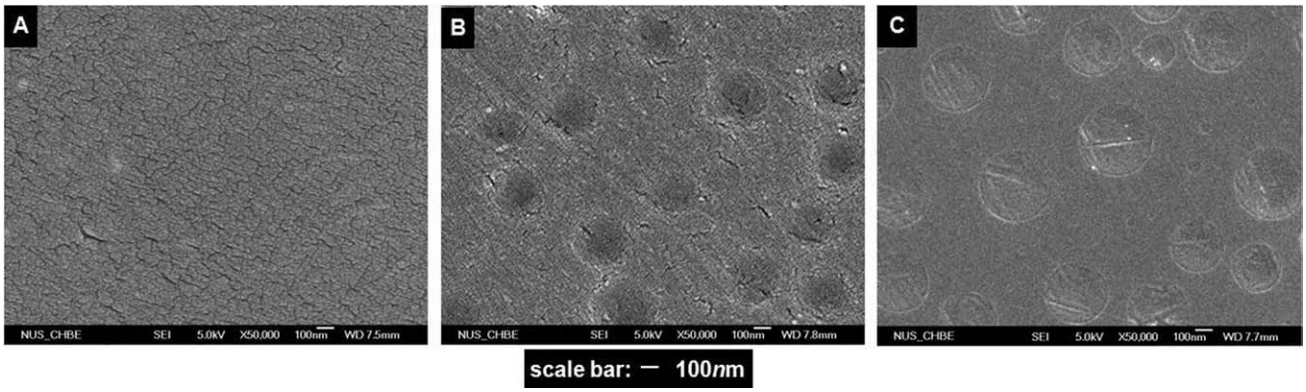

Figure 10. SEM pictures (a) the CD-grafted PAI dense composite membrane, (b) PAI/CD mixed matrix membrane with 5 wt % β-CD loading, and (c) PAI/CD mixed matrix membrane with 10 wt % β-CD loading.

chemical reaction between the amine group m-XDA-β-CD and the imide group of the PAI membrane, as proposed in Figure 4. The resultant amide bonding immobilizes β-CD structures strongly to prevent their agglomeration on the membrane surface. This reaction is confirmed by FTIR characterization as discussed in the following session.

The effect of surface modification time on PAI asymmetric membranes

Since dense flat membranes generally have very low fluxes and limited applications, we explore the feasibility of applying the newly developed surface modification technology to asymmetric membranes. Asymmetric membranes with high fluxes are much desirable and economical in industrial applications if the membrane selectivity is not compromised. Two factors are important to meet the mission: namely, (1) the development of asymmetric membranes with desirable substrate morphology and (2) the success of grafting m-XDA-CD upon the membrane surface. PAI asymmetric membranes were therefore fabricated from various dope concentrations and then grafted with m-XDA-CD with different modification time.

Figure 11 shows the pervaporation performance of grafted PAI asymmetric membranes as a function of modification time. The PAI asymmetric substrate is fabricated from a PAI 26 wt % NMP solution. As can be seen, all modified asymmetric membranes have higher fluxes compared to the modified dense membranes, which is mainly attributed to the thin thickness of the dense-selective layer of the asymmetric membrane and its substructure's porosity. The total butanol flux increases sharply within the initial 30-min modification with the highest flux value of 12.4 g/m^2/h, then starts to decrease with an increase in modification time. Finally it drops to 3.8 g/m^2/h at 5-h modification. No obvious change is observed if the modification time is longer than 5 h. On the other hand, the separation factor increases sharply from 1.2 with the unmodified membrane to a maximum value of 2.6 with 5-h modification and then show a slightly decreasing trend with further increase in modification time.

The enhanced separation factor is attributed to the molecular selective layer of CD-grafted upon the membrane surface. Generally speaking, the more CD deposition on the membrane surface, the higher the separation performance should be achieved. However, since the above CD grafting reaction (imide-amide conversion) is reversible as shown in Figure 4,[27] a lower degree of reaction may be resulted if the modification time is longer than 5 h. This may lead to a less CD amount grafted on the membrane surface and result in a lower separation factor. Another possible reason is due to the random cavity directions of grafted CDs. As a result, there exists an optimal CD content grafted on the asymmetric membrane for high separation of butanol isomers.

As to the up-and-down trend of the total butanol flux with an increase in the modification time, there exist two main factors: the bigger cavity size of grafted CD and the effect of m-XDA induced cross-linking reaction. The first factor plays determining roles to enhance butanol flux initially if the dense-selective layer is thin with minimal defects; while the second factor and other aforementioned factors such as reversible reaction are the main forces for the declined flux. As a result, the flux increases and then decreases with an increase in surface modification time.

The measurement of grafted CD amount on membrane surface as a function of reaction time may be characterized

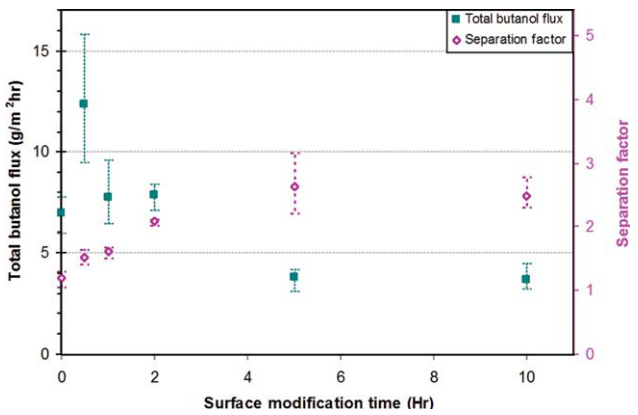

Figure 11. Pervaporation performance of the CD-grafted PAI asymmetric membranes as a function of modification time (the PAI asymmetric membrane was fabricated from a PAI 26 wt % NMP solution).

[Color figure can be viewed in the online issue, which is available at wileyonlinelibrary.com.]

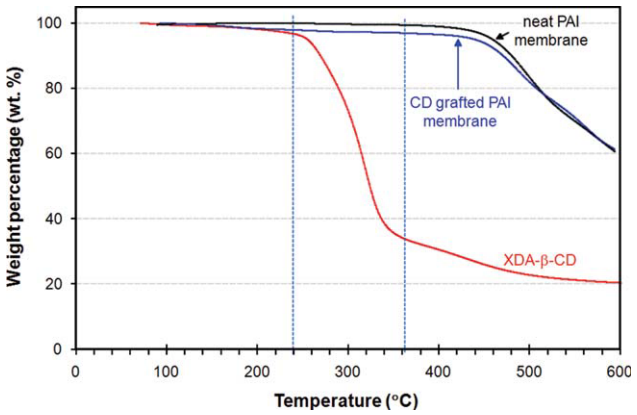

Figure 12. TGA characterization of m-XDA-β-CD, neat PAI membrane, and the CD-grafted PAI membranes.

[Color figure can be viewed in the online issue, which is available at wileyonlinelibrary.com.]

by TGA to support the above argument. Figure 12 illustrates the basic principle of this study. According to the TGA curve, the main thermal degradation of pure m-XDA-β-CD occurs in a temperature range of 240 to 360°C where there is a weight loss of 56 wt %. In contrast, the plain PAI membrane shows almost negligible thermal degradation (0.50 wt %) during this temperature range. Assuming pure and grafted m-XDA-β-CD are of the similar thermal decomposition behavior, a comparison of weight loss between the m-XDA-β-CD-grafted and plain PAI membranes during this temperature range would give the amount of grafted m-XDA-β-CD on the membrane surface by the relationship expressed as follows:

$$\Delta m_{\text{total}}(\text{mg}) = (m_{\text{total}} - m_{\text{CD}}) \cdot G_{\text{membr}} + m_{\text{CD}} \cdot G_{\text{CD}} \qquad (2)$$

here Δm_{total} is the total weight loss in this temperature range obtained from the TGA curve, m_{total} and m_{CD} refer to the total membrane weight and the grafted CD weight on the membrane surface, respectively, while G_{membr} and G_{CD} are the percentages of weight loss of neat PAI membrane and pure m-XDA-β-CD, respectively. The amount of grafted CD per unit membrane area is then calculated according to the Eq. 2 since all TGA samples of the CD-grafted membranes are prepared with the same membrane areas. Figure 13 shows the estimated grafted CD amount (with error bars) on membrane surface under various modification times calculated from TGA results. As mentioned above, the surface grafting by m-XDA-β-CD on PAI membrane is a time-dependent process. The TGA results illustrate that the transformation of imide to amide is triggered within 30 min. The imide to amide conversion may reverse after roughly 1 h reaction, consistent with the amount change of grafted CD (i.e., increasing initially and decreasing later). This up and down trend is a strong proof of the reaction equilibrium as shown in Figure 4, indicating the maximum degree of chemical reaction is achieved at around 1 h.

The TGA data can also be used to roughly calculate how many layers of CD molecules deposited on the membrane surface. This is due to the fact that the grafted CD amount per membrane surface has been measured using TGA, which is assumed to be a mg/cm^2. One can easily translate it to the number of CD molecules per unit area since the molecular weight of grafted m-XDA-β-CD is 1238 g/mol. The occupied surface area of a grafted CD molecule can be roughly calculated according to the outer periphery diameter of β-CD of about 15.4 Å.[41] As a result, the total available surface area of CD molecules on a unit membrane area (n) is a product of number of CD molecules per membrane area and the surface area of each CD molecule, which can be mathematically expressed as the following:

$$n = \left[\pi\left(\frac{15.4\cdot 10^{-8}}{2}\right)^2 \text{cm}^2\right] \cdot \left[\frac{a\cdot 10^{-3}\text{g/cm}^2}{1238\text{g/mol}}\right] \cdot \left[6.02\cdot 10^{23}\text{mol}^{-1}\right] \qquad (3)$$

Equation 3 can be further rewritten as follows:

$$n = 9057 \cdot a \qquad (4)$$

Since the total available CD surface area deposited on a unit membrane surface area is known, n can also be considered as the number of CD molecular layers on a unit membrane surface if the n value is bigger than 1. The calculated a value of CD-grafted PAI asymmetric membranes varies from 0.03 to 0.05 mg/cm^2 as shown in Figure 13, this implies the number of CD molecular layers on membrane surface is approximately about 270–450 layers. If we assume all CDs are grafted on the polymer chains are neatly arranged inside the polymer matrix, the molecular layer grafted with CD corresponds to 21–36 nm depth because each CD has a cavity height of 0.79 Å.[43] However, we must realize there are other factors not taken into account in this simply calculation: first, we didn't consider the impurity exist during CD grafting reaction, such as m-xylenediamine; second, the CD-grafted can′t be arranged inside the polymeric matrix in such a neat way.

To prove the existence of the cross-linking reaction, we have carried out solubility tests and DSC tests of the original PAI membrane and modified PAI membranes. The results

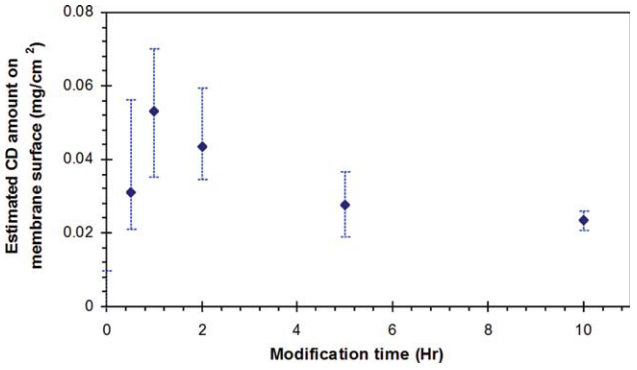

Figure 13. Estimated m-XDA-β-CD amount on the membrane surface of the CD-grafted PAI membranes as a function of modification time.

[Color figure can be viewed in the online issue, which is available at wileyonlinelibrary.com.]

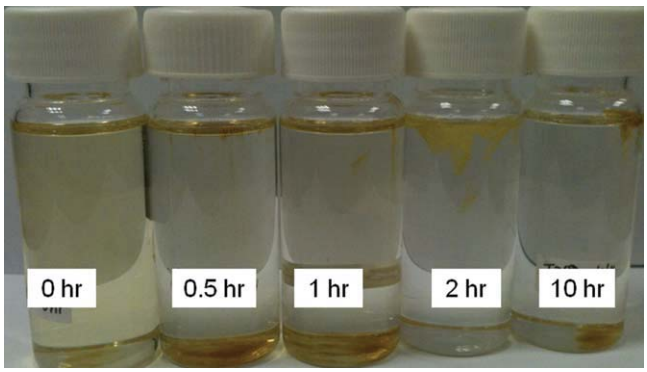

Figure 14. Solubility tests in solvent NMP of the CD-grafted PAI asymmetric membranes modified with m-XDA-β-CD for varied times.

[Color figure can be viewed in the online issue, which is available at wileyonlinelibrary.com.]

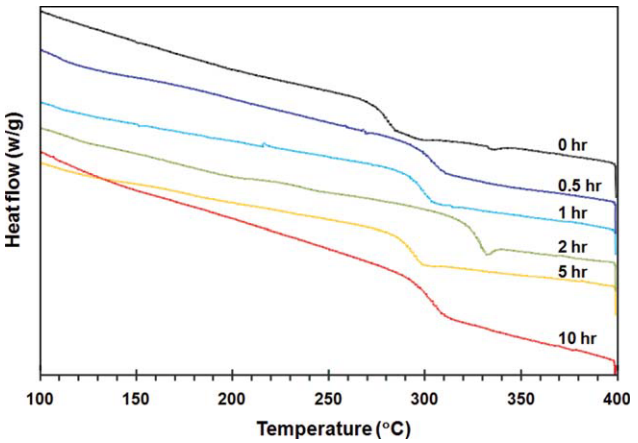

Figure 15. DSC curves of the CD-grafted PAI asymmetric membranes modified with m-XDA-β-CD for varied times.

[Color figure can be viewed in the online issue, which is available at wileyonlinelibrary.com.]

are shown in Figures 14 and 15, respectively. Solubility tests show the original PAI membrane can dissolve in NMP completely within 10 min, while the modified membranes only dissolve partially. The membrane modified for 2 h is of the worst solubility in NMP. The DSC results also show that the modified films are all of higher T_gs as compared to the original one, and the one with 2 h modification is of the highest T_g. It is believed the cross-linking reactions reduce solubility and result in higher T_g values.[44–46]

FTIR is also performed to confirm the proposed reaction mechanism as shown in Figure 4. Figure 16 demonstrates FTIR spectra of the CD-grafted PAI membranes with varied modification times. Bands at around 1782 cm^{-1} (attributed to C=O asymmetric stretch of imide groups), 1738 cm^{-1} (attributed to C=O symmetric stretch of imide groups), and 1328 cm^{-1} (attributed to C—N stretch of imide groups) are typical imide peaks in the original PAI membrane.[42,47] However, since the polymer PAI contains amide group itself before the CD modification, the amide peaks are also present even the modification time is 0. However, the amide

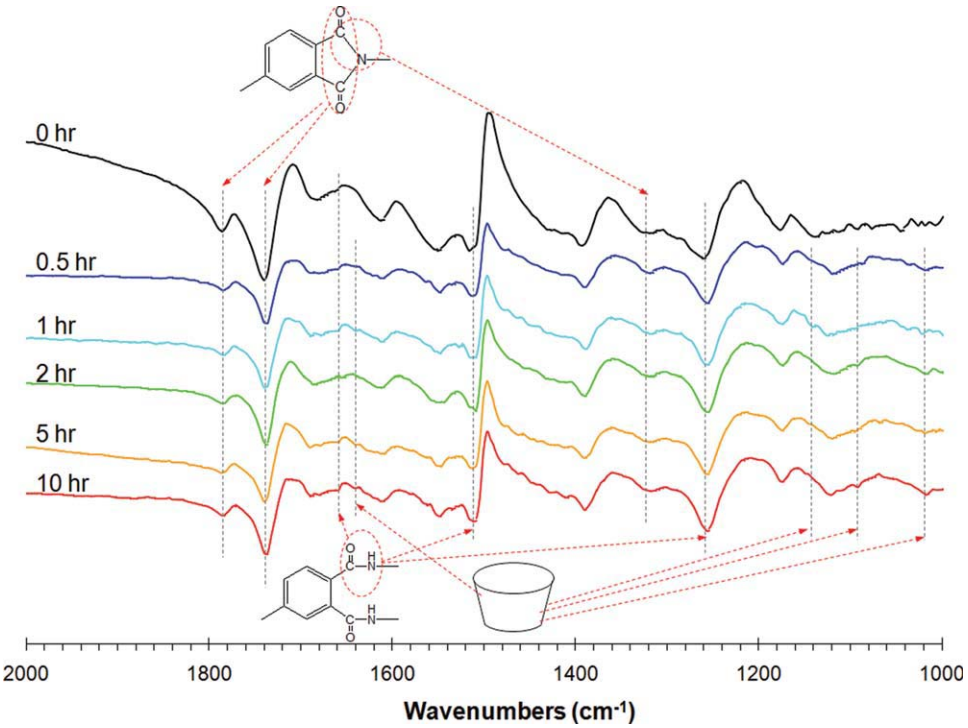

Figure 16. FTIR characterization of the CD-grafted PAI asymmetric membranes modified with m-XDA-β-CD for varied times.

[Color figure can be viewed in the online issue, which is available at wileyonlinelibrary.com.]

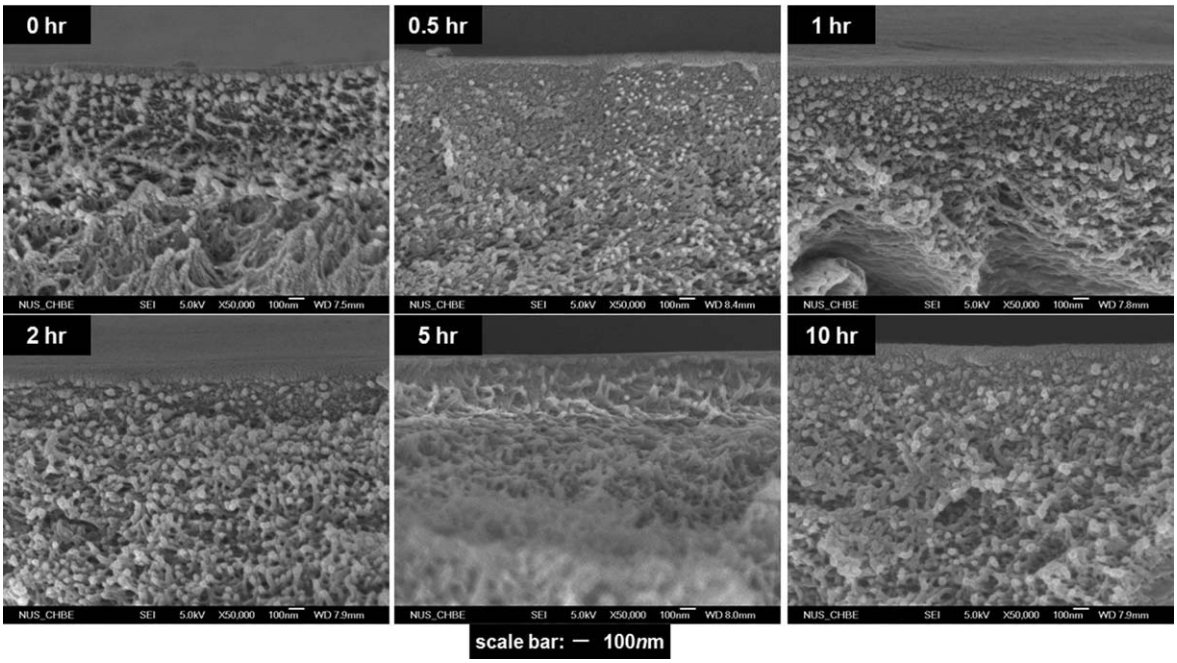

Figure 17. SEM images of the cross-section morphologies of the CD-grafted PAI asymmetric membranes modified with m-XDA-β-CD for varied times.

intensity changes with the modification time are still reflected by FTIR spectra. The characteristic imide peaks gradually decreases, while the characteristic bands for amide groups, namely, 1660 cm^{-1} (C═O stretching of amide groups) and 1512 cm^{-1} (N─H stretching) and 1260 cm^{-1} (CNH) increase progressively with increasing modification time.[27,47]

We can also observe the typical bands of CD rings although the amount of grafted CD is very little compared to the polymer chain content and its corresponding intensity is relatively low. The O─H bending vibration of the grafted CD occurs at about 1640 cm^{-1} and C─O─C characteristic stretching vibration appears at around 1145, 1095, and 1020 cm^{-1}. For membranes with lower CD content, the absorbance of these peaks may become weak and concealed by the stronger featuring peak of PAI. The FTIR results testify the conjugation of m-XDA-β-CD to the polymer chains via the amide formation between the amine of CD and the imide of the polymer backbone. By carefully comparing the amide stretching peaks in the composite membranes, it is found that increasing reaction time also results in some blue shifts of the amide peaks.[47,48] For example, the CNH peaks shift from 1260 cm^{-1} to 1254 cm^{-1}, which may arise from a higher density of hydrogen bonds in heavily amide groups.

Figure 17 shows the membrane morphologies as a function of modification time by means of FESEM. The FESEM images at 50,000 magnifications give a clear view of the top skin layer and show that the dense layer apparently becomes thicker and denser with an increase in modification time. The morphology evolution tallies well with the cross-linking effect of m-XDA.

The pervaporation performance of CD-grafted PAI asymmetric membranes prepared from different dope concentrations

The dope concentration for casting the PAI substrate membranes is an important parameter because it affects membrane morphology and plays an important role determining the separation performance of the resultant asymmetric membranes. Understanding their relationship would enable us to tailor the final PAI-CD composite membrane for pervaporation applications. Generally, concentrations near or higher than the critical value of polymer solutions are chosen for pervaporation membranes in order to make sure that the resultant membrane has less defects and possibly has a "quasi-dense" skin layer suitable for pervaporation.[19] The critical concentration of PAI/NMP solutions is about 26 wt %, obtained from viscosity-concentration curves,[19] where the viscosity of the polymer solution increases sharply, with the concentration at or higher than the critical value. In this study, the asymmetric membrane cast from dope solution of 26% concentration is called PAI 26%; the others are named analogically.

Figure 18 displays the effect of polymer concentration on total butanol flux of CD-grafted PAI asymmetric membranes, while Figure 19 shows the corresponding selectivity for isomer separation. The butanol flux decreases while the selectivity increases with an increase in polymer dope concentration. A high polymer concentration is principally beneficial to reduce the defects, but at the same time may cause a densified substrate. The separation factor of CD-grafted PAI membranes increases sharply with increasing concentration initially from 18 wt % to 22 wt % and then approaches an

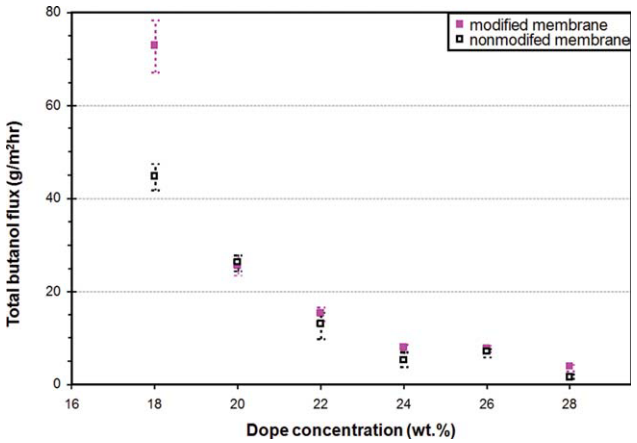

Figure 18. Total butanol flux of the CD-grafted PAI asymmetric membranes prepared from different dope concentrations.

[Color figure can be viewed in the online issue, which is available at wileyonlinelibrary.com.]

plateau with further increase in dope concentration. The initial sharp increase in selectivity may be resulted from intensified CD molecular packing and less defects of the skin layer in the membrane structure, while the slower increase in selectivity at higher polymer concentrations may be attributed to the increased substrate resistance and the fully packed CD layers on top of the membrane surface.

Generally, a dope concentration not less than the critical concentration of 26 wt % is recommended to cast unmodified PAI asymmetric membranes for pervaporation.[18] However, it is interesting to note that the CD-grafted PAI asymmetric membrane cast from a much lower dope concentration of about 22 wt % can be an effective pervaporation membrane for butanol isomer separation. This phenomenon is probably attributed to the following factors: (1) the grafted CD molecules may fill and seal the membrane surface defects and then accumulate on the surface; (2) the m-XDA-β-CD molecules may also be grafted on the membrane surface holes, not only tightening diffusion channels but also

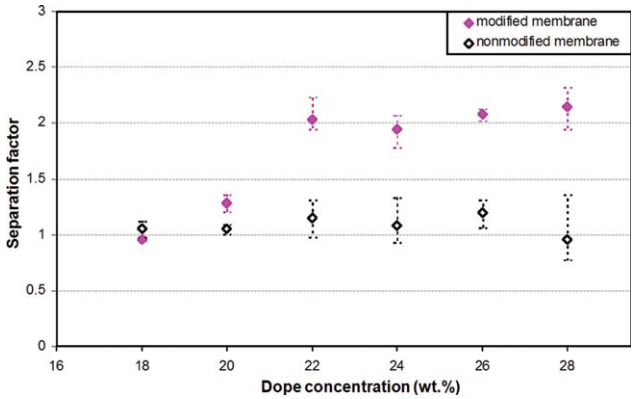

Figure 19. Separation factors of the CD-grafted PAI asymmetric membranes prepared from different dope concentrations.

[Color figure can be viewed in the online issue, which is available at wileyonlinelibrary.com.]

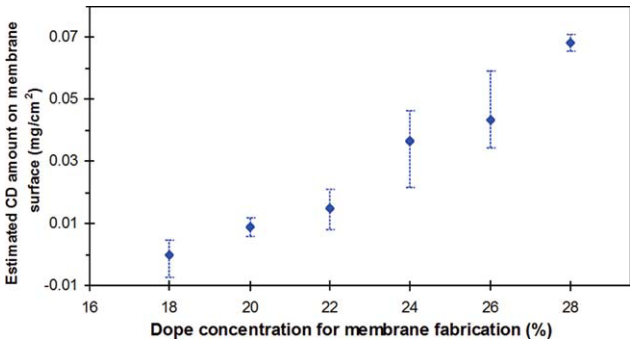

Figure 20. TGA characterization of the CD-grafted PAI asymmetric membranes prepared from different dope concentrations.

[Color figure can be viewed in the online issue, which is available at wileyonlinelibrary.com.]

increasing isomer selectivity as reported in the literature;[30] and (3) the minimization or tightening of the defects on membrane surface because of m-XDA induced cross-linking reactions. This speculation may be indirectly proved by the TGA results. As shown in Figure 20, we can see that the CD amount grafted on the membrane surface increases with an increase in dope concentration for the casting of asymmetric membranes.

Combing the effects from dope concentration and modification time, we can roughly integrate the overall experimental parameters to obtain the membrane with the best pervaporation performance for the separation of butanol isomers. Since 2-h modification time shows the most enhanced separation performance and a dope concentration at 22 wt % has both benefits of high flux and high separation performance, the most optimized PAI asymmetric membrane can be prepared from 22 wt % dope concentration with 2-h CD grafting modification on surface.

Conclusions

In this study, a novel CD-grafted PAI membrane is developed by grafting β-CD on the surface of the PAI asymmetric membrane. The as-fabricated membrane is characterized and investigated for butanol isomer separation through pervaporation with enhanced separation performance. The following conclusions can be made.

1. A new derivative of β-CD, m-XDA-β-CD, is used to graft β-CD on the membrane surface. The successful synthesis of m-XDA-β-CD is confirmed by the FTIR and TGA characterization. The molecular simulation implies m-XDA-β-CD may possess a lower inclusion ability of butanol molecules but a higher selectivity of the *n*-/*tert*-butanol isomer pairs compared to the original β-CD.

2. Compared to the PAI/CD MMM membrane made of physical mixing, a homogeneous morphology and an improved separation performance are obtained in the m-XDA-β-CD-grafted PAI membrane.

3. Because of the reversible reaction mechanism of the CD grafting modification, the modification time determines the CD amount on the membrane surface and the pervaporation performance of the resultant modified PAI membrane. FTIR and TGA characterizations are given to support this

speculation. TGA results indicate the maximum degree of reaction reaches at about 1 h.

4. The CD-grafted PAI asymmetric membranes show enhanced permeation fluxes as compared to the CD-grafted PAI dense membranes. The polymer concentration for the preparation of asymmetric membranes is an important factor affecting the pervaporation performance of the CD-grafted PAI asymmetric membrane. With the increase of the polymer concentration from 18% to 28%, the flux decreases while the separation factor improves significantly from 1.1 to about 2.3 for the CD-grafted PAI asymmetric membranes because of the increased CD amount on membrane surface and less membrane surface defects. A much lower polymer concentration (22 wt %) than the critical concentration (26 wt %) is found to be necessary on making a selective CD-grafted PAI asymmetric membrane.

5. The most optimal PAI asymmetric membrane can be prepared from 22 wt % dope concentration and with 2-h CD grafting modification on surface.

6. With CD immobilized on membrane surface, this newly developed PAI-CD composite membrane approach can be applied to all kinds of membrane morphologies, including the multilayer membranes and hollow fiber membranes, thus opens up a new way to prepare next-generation high-performance pervaporation membranes for isomer separation.

Acknowledgments

The authors thank A-Star (R-398-000-044-305 and R-279-000-288-305) and NRF CRP (R-279-000-311-281) for funding this research. Special thanks are due to Ms. Huan Wang, Mr. Peng Wang, and Mr. Kun Cheng for their help with the experiments.

Abbreviations

n-BuOH = *n*-butanol
t-BuOH = *tert*-butanol
CD = cyclodextrin
DSC = differential scanning calorimeter
NMP = *n*-methyl pyrrolidone
MMM = mixed matrix membrane
FTIR = Fourier transform infrared spectroscopy
FESEM = field emission scanning electron microscope
6FDA = 4,4′-(hexafluoro-isopropylidene)-diphthalic anhydride
6FpDA = 4,4′-(hexafluoro-isopropylidene)-dianiline
4MPD = 2,3,5,6-tetramethyl-1,4-phenylene-diamine
DABA = 3,5-diaminobenzoic acid
HMDA = hexamethylene diamine
mono-6-OTs-β-CD = 6-O-monotosyl-β-cyclodextrin
PAA = poly(acrylic acid)
PAI = polyamide-imide
PI = polyimide
PVA = poly(vinyl alcohol)
TGA = thermogravimetric analysis
m-XDA = m-xylenediamine
m-XDA-β-CD = m-xylenediamine-β-cyclodextrin

Notation

$\boldsymbol{a}$ = CD amount on the composite membrane (mg/cm^2)
d = average intersegmental distance of polymer chains (*d*-space)
G_{membr} = weight loss percentages of neat PAI membrane
G_{CD} = weight loss percentages of pure m-XDA-β-CD
J = permeate flux (g/m^2/h)
Δm_{total} = total weight loss of the PAI-CD composite membrane
m_{total} = total membrane weight
m_{CD} = mass of the grafted CD on the membrane surface
n = molecular layers grafted by the CD molecules
T_d = thermal decomposition temperature
T_g = glass transition temperature

Greek letters

α = separation factor

Literature Cited

1. Lue SJ, Liaw TH. Separation of xylene mixtures using polyurethane (PU)-zeolite composite membranes. *Desalination*. 2006;193:137.
2. McCandless FP, Downs WB. Separation of C-8 aromatic isomers by pervaporation through commercial polymer-films. *J Membr Sci*. 1987;30:111.
3. Wessling M, Werner U, Huang ST. Pervaporation of aromatic C-8-isomers. *J Membr Sci*. 1991;57:257.
4. Wegner K, Dong JH, Lin YS. Polycrystalline MFI zeolite membranes: xylene pervaporation and its implication on membrane microstructure. *J Membr Sci*. 1999;158:17.
5. Chen HL, Wu LG, Tan J, Zhu CL. PVA membrane filled beta-cyclodextrin for separation of isomeric xylenes by pervaporation. *Chem Eng J*. 2000;78:159.
6. Schleiffelder M, Staudt-Bickel C. Crosslinkable copolyimides for the membrane-based separation of p-/o-xylene mixtures. *React Funct Polym*. 2001;49:205.
7. Kusumocahyo SP, Sumaru K, Kanamori T, Iwatsubo T, Shinbo T. Synthesis and characterization of an ultrathin polyion complex membrane containing β-cyclodextrin for separation of organic isomers. *J Membr Sci*. 2004;230:171.
8. Yamasaki A, Mizoguchi K. Preparation of PVA membranes containing beta-cyclodextrin oligomer (PVA/CD Membrane) and their pervaporation characteristics for ethanol-water mixtures. *J Appl Polym Sci*. 1994;51:2057.
9. Yamasaki A, Iwatsubo T, Masuoka T, Mizoguchi K. Pervaporation of ethanol/water through a poly(vinyl alcohol)/cyclodextrin (PVA/CD) membrane. *J Membr Sci*. 1994;89:111.
10. Kusumocahyo SP, Kanamori T, Sumaru K, Iwatsubo T, Shinbo T. Pervaporation of xylene isomer mixture through cyclodextrins containing polyacrylic acid membranes. *J Membr Sci*. 2004;231:127.
11. Miyata T, Iwamoto T, Uracami T. Characteristics of permeation and separation for propanol isomers through poly(vinyl alcohol) membranes containing cyclodextrin. *J Appl Polym Sci*. 1994; 51:2007.
12. Miyata T, Iwamoto T, Uracami T. Characteristics of permeation and separation of xylene isomers through poly(vinyl alcohol) membranes containing cyclodextrin. *Macromol Chem Phys*. 1996;197:2909.
13. Touil S, Palmeri J, Tingry S, Bouchtalla S, Deratani A. Generalized dual-mode modeling of xylene isomer sorption in polyvinylalcohol membranes containing α-cyclodextrin. *J Membr Sci*. 2008;317:2.
14. Lue SJ, Peng SH. Polyurethane (PU) membrane preparation with and without hydroxypropyl-_-cyclodextrin and their pervaporation characteristics. *J Membr Sci*. 2003;222:203.
15. Peng FB, Jiang ZY, Hu CL, Wang YQ, Lu LY, Wu H. Pervaporation of benzene/cyclohexane mixtures through poly(vinyl alcohol) membranes with and without β-CD. *Desalination*. 2006;193:182.
16. Schneiderman E, Stalcup AM. Cyclodextrins: a versatile tool in separation science. *J Chromatogr B*. 2000;745:83.
17. Bender ML, Komiyama M. *Cyclodextrin Chemistry*. Berlin: Springer-Verlag, 1978.
18. Wang Y, Chung TS, Wang H, Goh SH. Butanol isomer separation using polyamide-imide/CD mixed matrix membranes via pervaporation. *Chem Eng Sci*. 2009;64:5198.
19. Wang Y, Jiang LY, Matsuura T, Chung TS, Goh SH. Investigation of the fundamental differences between polyamide-imide (PAI) and polyetherimide (PEI) membranes for isopropanol dehydration via pervaporation. *J Membr Sci*. 2008;318:217.
20. Wang Y, Goh SH, Chung TS, Peng N. Polyamide-imide/polyetherimide dual-Layer hollow fiber membranes for pervaporation dehydration of C1-C4 alcohols. *J Membr Sci*. 2009;326:222.

21. Teoh MM, Chung TS, Wang KY, Guiver MD. Exploring Torlon/P84 co-polyamide-imide blended hollow fibers and their chemical cross-linking modifications for pervaporation dehydration of isopropanol. *Sep Purif Technol*. 2008;61:404.
22. Yoshikawa M, Higuchi A, Ishikawa M, Guiver MD, Robertson GP. Vapor permeation of aqueous 2-propanol solutions through gelatin/Torlon® poly(amide-imide) blended membranes. *J Membr Sci*. 2004;243:89.
23. Higuchi A, Yoshikawa M, Guiver MD, Robertson GP. Vapor permeation and pervaporation of aqueous 2-propanol solutions through the Torlon poly(amide imide) membrane. *Sep Sci Technol*. 2005;40:2697.
24. Jonquières A, Dole C, Clément R, Lochon P. Synthesis and characterization of new highly permeable polyamideimides from dianhydride monomers containing amide functions: an application to the purification of a fuel octane enhancer (ETBE) by pervaporation. *J Polym Sci Part A Polym Chem*. 2000;38:614.
25. Hu Q, Marand E, Dhingra S, Fritsch D, Wen J, Wilkes G. Poly(amide-imide)/TiO_2 nano-composite gas separation membranes fabrication and characterization. *J Membr Sci*. 1997;135:65.
26. Jiang LY, Chung TS. β-Cyclodextrin containing Matrimid® nanocomposite membranes for pervaporation application. *J Membr Sci*. 2009;327:216.
27. Jiang LY, Chung TS. Homogeneous polyimide/cyclodextrin composite membranes for pervaporation dehydration of isopropanol. *J Membr Sci*. 2010;346:45.
28. Robertson GP, Guiver MD, Yoshikawa M, Brownstein S. Structural determination of Torlon (R) 4000T polyamide-imide by NMR spectroscopy. *Polymer*. 2004;45:1111.
29. Liu YY, Fan XD, Zhao YB. Synthesis and characterization of a poly(*N*-isopropylacrylamide) with β-cyclodextrin as pendant groups. *J Polym Sci Part A Polym Chem*. 2005;43:3516.
30. Zhou ZZ, Chung TS, Hatton AT. Effects of spacer arm length and benzoation on enantioseparation performance of β-cyclodextrin functionalized cellulose membranes. *J Membr Sci*. 2009;339:21.
31. Guo WF, Chung TS, Matsuura T, Wang R, Liu Y. Pervaporation study of water and *tert*-butanol mixtures. *J Appl Polym Sci*. 2004;91:4082.
32. Kacso I, Borodi G, Fărcas SI, Bratu I. Inclusion compound of vitamin B13 in b-Cyclodextrin Structural investigations. *J Phys Conf Ser*. 2009;182:012009.
33. Bocanegra-Diaz A, Mohallem NDS, Sinisterra RD. Preparation of a ferrofluid using cyclodextrin and magnetite. *J Braz Chem Soc*. 2003;14:936.
34. Zielske AG. Method for preparing 1,4-diaminoanthraquinones and intermediates thereof. US Patent 4746461, 1986.
35. Xiao YC, Lim HM, Chung TS, Rajagopalan R. Acetylation of β-cyclodextrin surface-functionalized cellulose dialysis membranes with enhanced chiral separation. *Langmuir*. 2007;23:12990.
36. van Leeuwen ME. Derivation of Stockmayer potential parameters for polar fluids. *Fluid Phase Equlib*. 1994;99:1.
37. Wijmans JG. Process performance = membrane properties + operating conditions. *J Membr Sci*. 2003;220:1.
38. Reichardt C. *Solvents and Solvent Effects in Organic Chemistry*, 2nd ed. Weinheim: VCH, 1988.
39. Hansen CM. *Hansen Solubility Parameters: A User's Handbook*. Boca Raton, FL: CRC Press, 2007.
40. Huang RYM, Jarvis NR. Separation of liquid mixtures by using polymer membranes. II. Permeation of aqueous alcohol solutions through cellophane and poly(vinyl alcohol). *J Appl Polym Sci*. 1970;14:2341.
41. Lu J, Mirau PA, Tonelli AE. Chain conformations and dynamics of crystalline polymers as observed in their inclusion compounds by solid-state NMR. *Prog Polym Sci*. 2002;27:357.
42. Qiao XY, Chung TS. Diamine modification of P84 polyimide membranes for pervaporation dehydration of isopropanol. *AIChE J*. 2006;52:3462.
43. Bressole F, Audran M, Pham TN, Vallon JJ. Cyclodextrins and enantiometric separations of drugs by liquid chromatography and capillary electrophoresis: basic principles and new developments. *J Chromatogr B*. 1996;687:303.
44. Shao L, Chung TS, Goh SH, Pramoda KP. Polyimide modification by a linear aliphatic diamine to enhance transport performance and plasticization resistance. *J Membr Sci*. 2005;256:46.
45. Shao L, Liu L, Cheng SX, Huang YD, Ma J. Comparison of diamino cross-linking in different polyimide solutions and membranes by precipitation observation and gas transport. *J Membr Sci*. 2008;312:174.
46. Fox TG, Loshaek S. Influence of molecular weight and degree of cross-linking on the specific volume and glass temperature of polymers. *J Polym Sci*. 1955;15:371.
47. DiMarzio EA. The second-order transition of rubber. *J Res Nat Bur Stand Sect A Phys Chem*. 1964;68A:611.
48. Powell CE, Duthie XJ, Kentish SE, Qiao GG, Stevens GW. Reversible diamine cross-linking of polyimide membranes. *J Membr Sci*. 2007;291:199.
49. Zhou ZZ, Xiao YC, Hatton TA, Chung TS. Effects of spacer arm length and benzoation on enantioseparation performance of beta-cyclodextrin functionalized cellulose membranes. *J Membr Sci*. 2009;339:21.

Manuscript received Apr. 20, 2010, and revision received Jun. 24, 2010.